Correlation Between Surface Engineering and Deformation Response of Some Natural Polymer Fibrous Systems

Narcisa Vrinceanu[1], Mirela Iorgoaiea Guignard[2], Christine Campagne[3], Stephane Giraud[4], Raluca Ioana Prepelita[5]
Diana Coman[1], Valentin Dan Petrescu[1], Dan Dumitru Dumitrascu[1], Noureddine Ouerfelli[6], Mirela Petruta Suchea[7]

[1]Lucian Blaga University of Sibiu, Faculty of Engineering, Sibiu ROMANIA

[2]Gheorghe Asachi Technical University of Iaşi, Iasi ROMANIA

[3]University Lille Nord France, Roubaix FRANCE and Gemtex, Ensait, Roubaix FRANCE

[4]ENSAIT, Lab Genie Mat Text GEMTEX, Roubaix FRANCE

[5]University of Medicine and Pharmacy of Iaşi, Faculty of Medicine, Iasi ROMANIA

[6]Imam Abdulrahman Alfaisal University, College of Science, Dammam SAUDI ARABIA and Université de Tunis
El Manar, Institut Supérieur des Technologies Médicales de Tunis, Zouhaier Essafi Tunis TUNISIA

[7]Center of Materials Technology and Laser, School of Electrical Engineering, Heraklion GREECE and
National Institute for Research and Development in Microtechnologies (IMT-Bucharest), Bucharest ROMANIA

Correspondence to:
Narcisa Vrinceanu email: vrinceanu.narcisai@ulbsibiu.ro

ABSTRACT
Surfaces of bamboo derived cellulosic fibrous systems have been modified by air-plasma treatment. Their deformational response was studied to establish the relationship between their three-dimensional profile and permanent deformation as a measure of their comfort properties since the fibrous system made of natural polymer comes into contact with the skin. The composite should have a permanent deformation close to zero, in order to be, in terms of dimensions, as stable as possible. By analyzing the area of 1 cm^2 using a Universal Surface Tester (UST), different 3D surface diagrams and surface roughness values were obtained. This type of surface investigation provides relevant information about the permanent deformation response of the studied surface, for comfort purposes. The deformation responses and roughness levels were studied (the roughness being the parameter quantifying the 3D geometry of the systems surface). The effect of air-plasma surface modification on the deformation response of bamboo derived cellulosic fibrous systems and optimization of their 3D surface structure to enhance comfort-related properties proved to be substantial. The surface modifications induced by air-plasma treatment are in a good correlation with the mechanical behavior. As expected, the roughness levels of samples studied using ball sensors are higher than those of specimens scanned using a papillary sensor. Knitted polymer fibrous matrix T1 shows a roughness level of 773 μm resulting from analyses using the ball sensor, while using the papillary sensor it was 102 μm, 86.8% less than before. The analysis of the dimensional stability of knitted polymer fibrous systems was performed by scanning with the papillary sensor, since it provides information comparable with human perception concerning the architecture of the sample surfaces.

Keywords: fibrous composite; bamboo fibers; permanent deformation; functionalization; surface geometry; air plasma treatment; roughness level; elastic deformation; total deformation; peaks density; dimensional stability; papillary sensor; ball sensor

INTRODUCTION
Natural polymer fibrous systems with three-dimensional (3D) surface textures have major potential to be used as medical supports. Their massaging performance can be quantified by means of surface tests. The 3D surface structure should be analyzed in order to measure the massaging effect since the massaging polymer fibrous supports come into direct contact with the skin.

3D surface structure characterization can be achieved by roughness analyses and by dimensional stability analysis of knitted polymer fibrous systems, as well as their permanent, elastic and total deformation. These analyses can be performed using a Universal Surface Tester (UST). The roughness of a polymer fibrous system is calculated using cross-section profiles resulting from their analyses with UST. According to ISO 4287 Standard [1], the massaging effect is directly proportional to the roughness level. The dimensional stability of polymer fibrous systems can be quantified by the permanent, elastic and total deformation of the 3D profile. The roughness level of polymer fibrous systems increases as their deformation diminishes and the 3D surface reverts to the initial state, when used. Consequently, the dimensional stability of polymer fibrous matrices is defined by an ideally zero permanent deformation and a small elastic deformation.

The present work studies the effect of air-plasma surface modification on the deformation response of bamboo derived cellulosic fibrous systems and predicts the optimization of their 3D surface structure to enhance their comfort-related properties. Successful experiments will open possibilities for the use of air-plasma treatment not only to sterilize textile medical supports surfaces but also to improve comfort on contact with the skin. This will have a strong impact in medical applications of bamboo derivate cellulosic fibrous systems. To achieve this, bamboo yarn knitted textile supports with a 3D surface geometry were used. Activation of the textile support using air-plasma treatment was performed to increase the surface energy. Atmospheric plasma surface treatments promote adhesion by removing organic and inorganic surface contaminants. Atmospheric plasma is ideal for improving adhesion of a wide variety of materials used in the medical industry to clean surfaces, promote adhesive bonding and enable printing on polymers of all shapes and sizes. Reactive gases are diffused toward the surface under the influence of electric fields. Low molecular weight materials such as water, absorbed gases and fragments are removed to expose a clean, fresh surface. At the same time, a percentage of the reactive components in plasma with sufficient energy bond to the freshly exposed surface, changing the chemistry of the surface and imparting the desired functionalities. Air-plasma treatment leads to an improvement of comfort when used on medical textiles as well as a means to obtain sterile and contaminant-free surfaces. Plasma processing is a clean and dry technology which offers numerous advantages over the conventional chemical processes and it is considered to be more economical and environmentally friendly. Air-plasma treatment is intended to modify polymer surfaces using plasma, which is a mixture of charged particles (electrons and ions), excited atoms (free radicals and meta-stable molecules) and photons [2-10]. Plasma is formed when the gas (air in our case) between two electrodes is subjected to high voltage. During plasma treatment, the polymer is exposed to reactive species that interact with its surface, the result being chemical modifications at the surface level. These modifications depend on the nature of the polymer and the chemical composition of the plasma, as well as the treatment parameters [11-20].

MATERIALS AND METHODS
Materials
A knitted fabric with a tubular evolution and transfer pattern made of bamboo yarns with a fineness of Nm 24/1, 416.6 dTex, 374.4 Den, diameter of 80-100 µm, circular cross-section (Abtex International Ltd) was used. The physical-mechanical attributes are as follows: tensile strength at break (2.48 cN/dtex), fiber density 0.32 g/cm^3, breaking extension 24 percent. The fabric was produced on a Stoll flat electronic machine, gauge 18E. It results in a structure characterized by a 3D surface geometry created by the stitch transfers from the front bed to the rear. After knitting, the fabric was relaxed in a dry state and then washed in an ultrasonic bath (water, detergent and sodium carbonate), for 1 hour, at 60°C, in order to remove impurities [20-27].

Methods
Air Plasma Treatment
For air-plasma surface modification of bamboo derived cellulosic fibrous systems, "Coating Star with corona discharge" (Ahlbrandt System) equipment was used. The air-plasma surface modification constant parameters in our case were: speed (2 m/min), frequency (26 kHz), voltage (15 kV), electrode length (0.5 m), and distance between electrodes (2 mm). Air was the choice as plasma gas during the treatment. Samples with dimensions of ~15 × 15 mm^2 were subjected to an air-plasma treatment with different electrical powers: 0 (T1-reference), 300 W (T2), 700 W (T3), 1000 W (T4) and 1000 W (twice on the same side) (T5) [5]. As a result of air-plasma treatment, the surface topography should be consistently modified. The modified surfaces architecture was quantified according to ISO 4288 using a Universal Surface Tester (UST)(Innowep GmbH) laboratory device [2]. For scanning, two types of sensors (ball sensor and papillary) were used, and information concerning the 3D profiles (3D standard measurements) of these

surfaces was obtained. The surface roughness was also estimated for each sample.

RESULTS AND DISCUSSION

UST characterization of the T1-T5 samples (1x1 cm^2 area) using the two types of sensors, ball and papillary, is presented in *Figures 1-5*. A graphical example of a particular scan is shown in *Figure 6*.

Data regarding the permanent, elastic and total deformation as well as roughness were collected.

The test principle and color code in all the images is:
Scan 1 red: Scan with no load. Surface structure is continuously determined.
Scan 2 green: Scan on the same path with additional load 70 (mN) to determine total deformation.
Scan 3 blue: Scan on the same path with no load to determine the elastic deformation.
Permanent deformation = Scan 1- Scan 3
Elastic deformation = Scan 3- Scan 2;
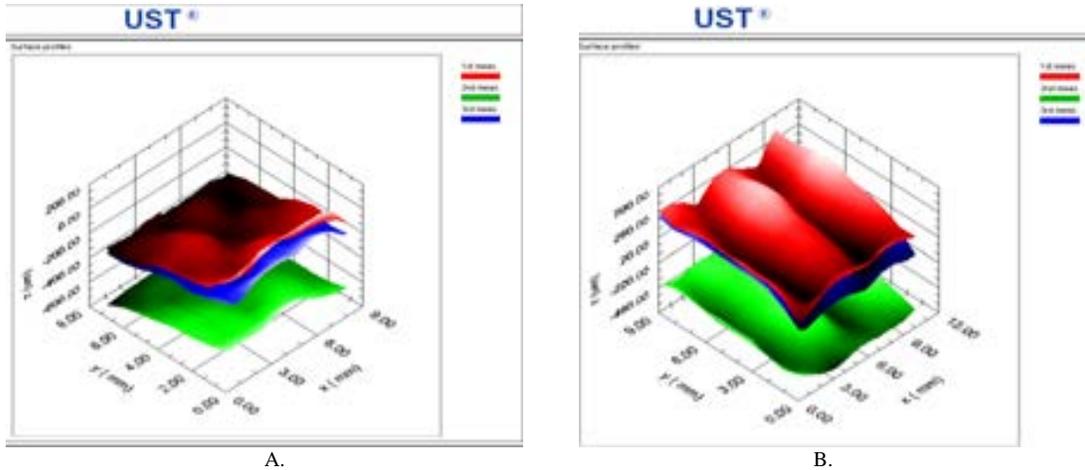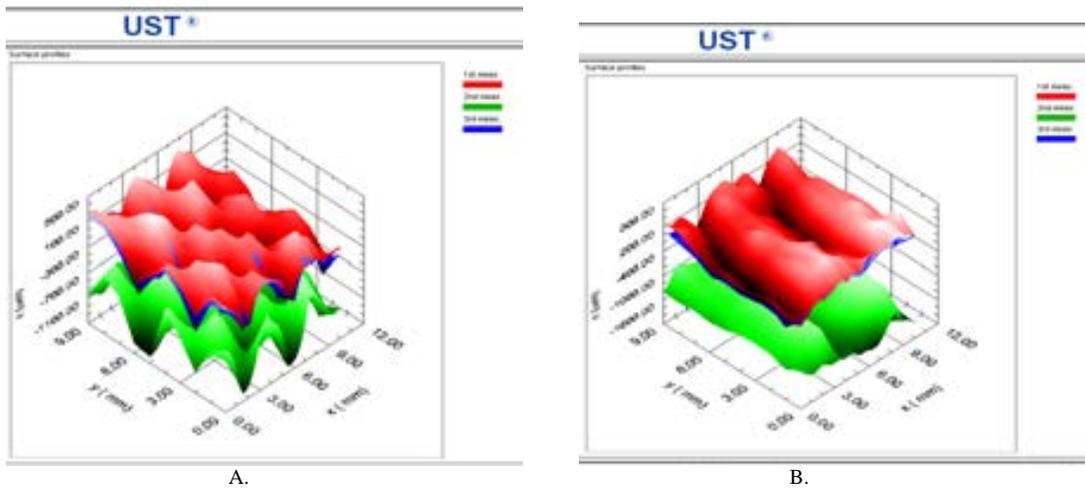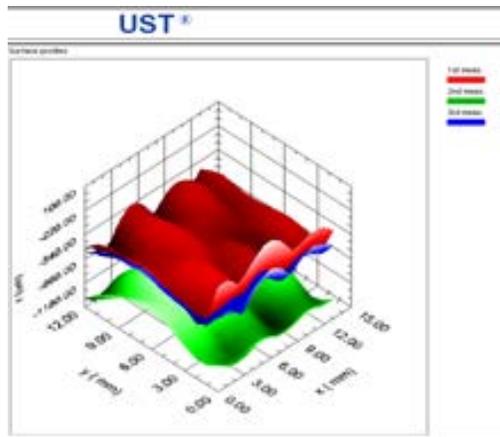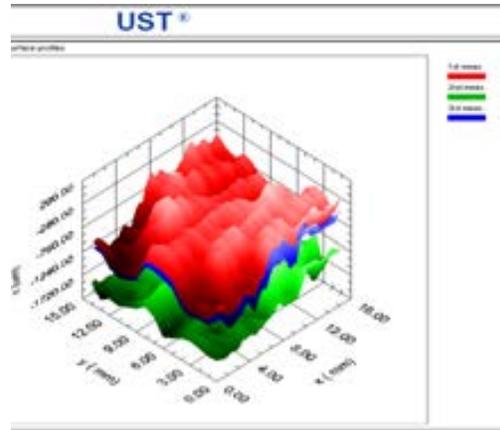Total Deformation = Scan 1- Scan 2;

FIGURE 1. Polymer fibrous knitted matrix T1: A) 3D image obtained with UST, using ball sensor (X$_{AXIS}$ 0-9 mm, Y$_{AXIS}$ 0-8 mm, Z$_{AXIS}$ 200 to -800 μm); B) 3D image obtained with UST, using papillary sensor. (X$_{AXIS}$ 0-12 mm, Y$_{AXIS}$ 0-9 mm, Z$_{AXIS}$ 400 to -600 μm).

FIGURE 2. Polymer fibrous knitted matrix T2: A) 3D image obtained with UST, using ball sensor (X$_{AXIS}$ 0-9 mm, Y$_{AXIS}$ 0-8 mm, Z$_{AXIS}$ 200 to -1200 μm); B) 3D image obtained with UST, using papillary sensor. (X$_{AXIS}$ 0-12 mm, Y$_{AXIS}$ 0-9 mm, Z$_{AXIS}$ 400 to -1200 μm).
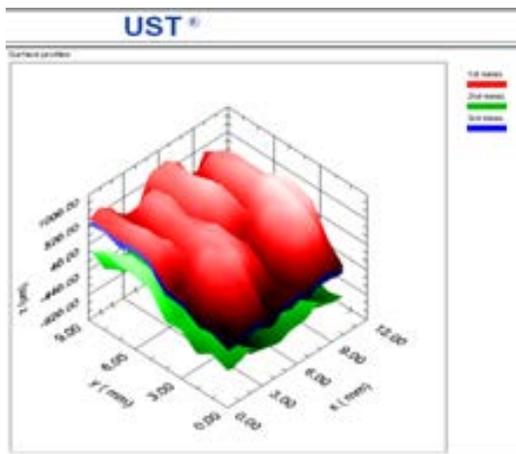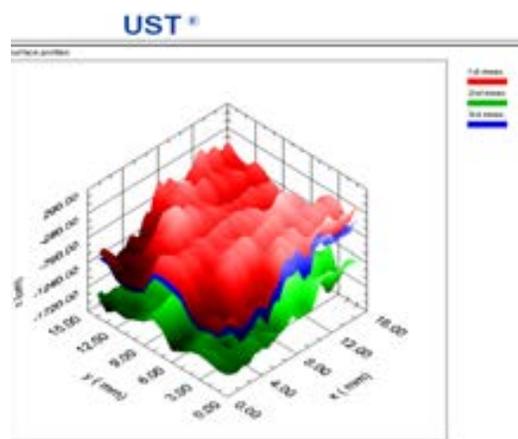
A.

B.

FIGURE 3. Polymer fibrous knitted matrix T3: A) 3D image obtained with UST, using ball sensor (X_{AXIS} 0-15 mm, Y_{AXIS} 0-12 mm, Z_{AXIS} 0 to -1200 μm); B) 3D image obtained with UST, using papillary sensor. (X_{AXIS} 0-16 mm, Y_{AXIS} 0-15 mm, Z_{AXIS} 200 to -1200 μm).

A.

B.

FIGURE 4. Polymer fibrous knitted matrix T4: A) 3D image obtained with UST, using ball sensor (X_{AXIS} 0-12 mm, Y_{AXIS} 0-9 mm, Z_{AXIS} 1000 to -1000 μm); B) 3D image obtained with UST, using papillary sensor. (X_{AXIS} 0-16 mm, Y_{AXIS} 0-15, mm Z_{AXIS} 200 to -1200 μm).
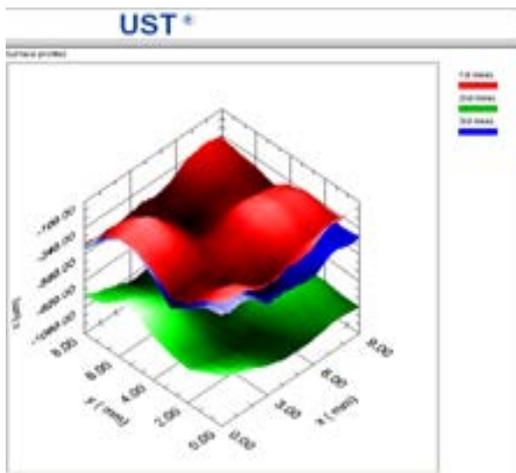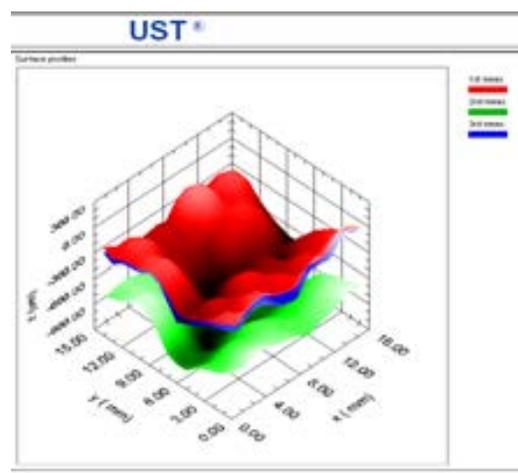

A.

B.

FIGURE 5. Polymer fibrous knitted matrix T5: A) 3D image obtained with UST, using ball sensor (X_{AXIS} 0-9 mm, Y_{AXIS} 0-8 mm, Z_{AXIS} -200 to -1200 μm μm); B) 3D image obtained with UST, using papillary sensor. (X_{AXIS} 0-16 mm, Y_{AXIS} 0-15 mm, Z_{AXIS} 200 to -1000 μm).
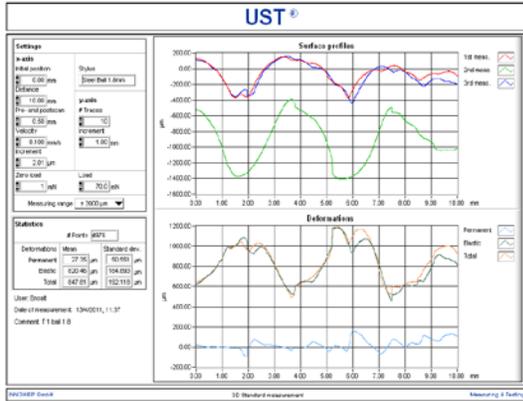
FIGURE 6. Example of surface analysis of T1 sample with ball sensor on a base of length of 10 mm, with 3 scans.

The first scan is performed on a length of 1 cm, representing a base length. It returns on the same base line, with pre-tension of the sensor of 70 mN during the second scan, and in the third scan the sensor is making its way back, without any pre-tension on the same line. Then the sensor goes to the right by 1 mm. Ten measurements are gathered on the 10 length bases, representing the analysis of a surface area of 1 cm². The studied surface was 1 cm² for knitted polymer fibrous systems T1, T2, T3, T5, and 4 cm² for the T4 sample. UST was used also to estimate the surface roughness of the studied samples. An example of roughness calculation is presented in *Figure 7*.
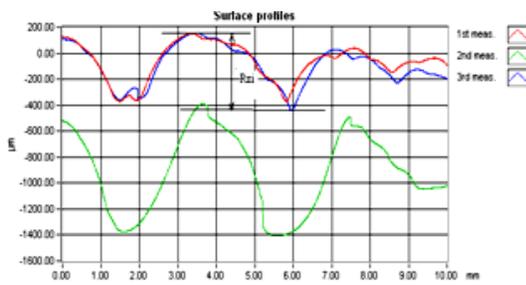

FIGURE 7. Example of calculus for roughness values on a base length l_b.

As shown in *Figure 7,* R_{zi} roughness values were estimated for each of the five different types of polymer fibrous systems. The mean value for roughness R_z corresponding to each sample was calculated with the mathematical relation:

$$R_z = \frac{1}{n_{l_b}} \times \sum_0^{l_b} R_{zi} \qquad (1)$$

where:

R_{zi} –the maximal heights calculated for every base length, as can be seen in *Figure 7*.

l_b- base length;

n_{lb}- number of base lengths.

The calculated values of surface roughness for the T1-T5 samples obtained with UST, using the ball sensor, are presented in *Table I,* and those achieved by analysis using the papillary sensor are presented in *Table II*.

TABLE I. The roughness values of the 5 samples analyzed using the ball sensor.

Base lengths l_b	The tally of roughness levels associated with the 5 types of samples analyzed with the ball sensor Rzi [µm]				
	T1	T2	T3	T4	T5
lb1	550	600	200	1090	630
lb2	800	900	800	860	900
lb3	800	950	1020	940	580
lb4	900	850	1060	850	910
lb5	650	750	950	960	920
lb6	780	850	450	820	740
lb7	940	700	570	800	880
lb8	860	700	520	790	600
lb9	750	650	650	650	840
lb10	700	780	800	720	950
lb11				1180	
lb12				950	
lb13				1000	
lb14				900	
lb15				900	
lb16				860	
lb17				920	
lb18				870	
lb19				850	
lb20				950	
Rz	773	773	702	893	795

TABLE II. The roughness values of the 5 samples analyzed using the papillary sensor.

Base lengths l_b	The tally of roughness levels associated with the 5 types of samples analyzed with the papillary sensor Rzi [µm]				
	T1	T2	T3	T4	T5
l_b	130	100	330	730	200
lb2	50	200	170	750	240
lb3	120	280	200	770	230
lb4	100	300	230	630	240
lb5	170	310	260	700	170
lb6	120	380	270	690	170
lb7	80	390	200	670	310
lb8	50	340	200	750	190
lb9	110	290	180	820	200
lb10	90	210	200	690	210
lb11				650	
lb12				650	
lb13				670	
lb14				640	
lb15				530	
lb16				610	
lb17				600	
lb18				700	
lb19				1000	
lb20				1130	
Rz	102	280	224	719	216

Table I and *Table II* show the 10 length bases' (lb1-b10) measured roughness values (for a 10 mm width of the surface of samples T1, T2, T3, T5, and 20 for T4. The peak density or number of peaks/cm^2, can be calculated by direct counting on the surface of the systems, using a template of 1 cm^2 placed on the specimens, or from *Figures 1 b-5 b*, showing 3D images of polymer fibrous knitted structures, obtained through scanning with the papillary sensor (similar to human perception).

The complete UST characterization results of the analyzed samples are centralized in *Table III* and *Table IV*.

TABLE III. Permanent, elastic and total deformation and roughness levels for the 5 types of samples analyzed with the ball sensor.

Spls	Ball sensor						Roughness level Rz (µm)
	Perm. def. (µm)		Elast. def. (µm)		Tot. def. (µm)		
	Avg	Std. dev.	Avg	Std. dev.	Avg	Std. dev.	
T1	77.03	56.07	814.28	176.9	891.31	175.99	773
T2	221.4	111.99	1202.6	384.09	1424.1	381.28	773
T3	133.1	50.69	682	270.76	815.17	282.9	702
T4	143.1	79.81	779.59	191.89	922.77	232.23	894
T5	163.3	66.64	839.46	197.06	1002.7	221.2	795

TABLE IV. Permanent, elastic and total deformation and roughness level for the 5 types of samples analyzed with the papillary sensor.

Spls	Papillary sensor						Roughness level Rz (µm)	Peaks density (peaks number/cm^2)
	Perm. def. (µm)		Elast. def. (µm)		Tot. def. (µm)			
	Avg	Std. dev.	Avg	Std. dev.	Avg	Std. dev.		
T1	67	50.94	408.4	36.89	475.43	64	102	1
T2	56.7	48.86	625.16	82.09	681.92	82.3	280	3
T3	86	80.89	559.72	113.27	665.71	170	246	2
T4	45.8	22	478.06	120.46	523.87	118.9	719	4
T5	70.1	57.267	584.14	69.65	654.25	89.4	216	5

In *Table IV* it is observable that the highest density of the peaks belongs to the T4 and T5 samples, so these specimens show the least deformation.

Figures 8-10 present the variation of the UST estimated parameters of 3D surface texture using the ball and papillary sensors for samples T1-T5 as well as the variation of permanent deformation with roughness level. As can be seen, samples T1 and T2, although having similar roughness, show extreme values of the permanent deformation, while the other samples show a permanent deformation in the same range.
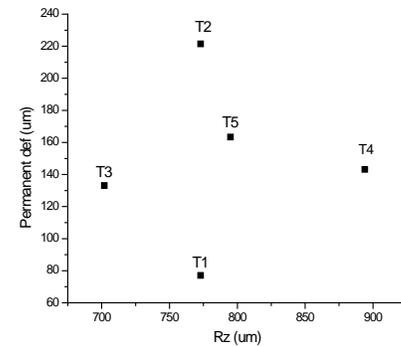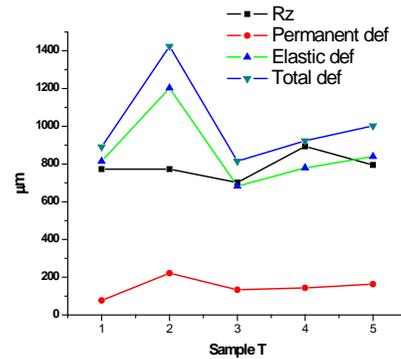

FIGURE 8. Ust estimated parameters of 3d surface texture using the ball sensor for the analyzed samples t1-t5 and variation of permanent deformation with roughness level.
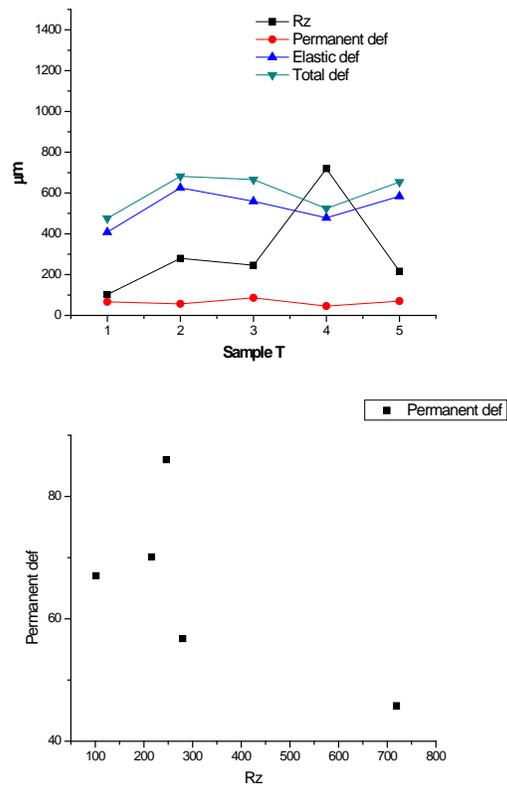
FIGURE 9. UST estimated parameters of 3D surface texture using the papillary sensor for the analysed samples T1-T5 and variation of permanent deformation with roughness level.
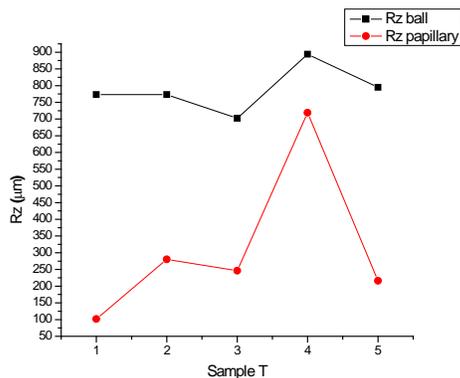

FIGURE 10. Roughness level of the 5 types of bamboo derived cellulosic fibrous systems whose surfaces were analysed with the ball and papillary sensors.

This fact can be explained by the initial effect of plasma treatment on bamboo fibers, consisting in surface chemical modification and the removal of surface contaminants by ablation. After the removal of surface contaminants and other weakly bonded species, the plasma treatment effect is gentler, almost linear.

In *Figure 10*, one can see that the roughness level of the samples analyzed with the ball sensor is higher than when measured with the papillary sensor. This is because the smaller the sensor diameter, the more accurate the information regarding the profile of knitted systems. Sample T1 has the roughness level measured with the ball sensor of 773, compared with the value of 102 obtained by analyzing the same sample with the papillary sensor (86.8% difference).

The dimensional stability analyses of polymer fibrous systems show that the lowest value of permanent deformation is obtained for sample T4 (45.81 μm), and compared with the other structures, this has a low total deformation as well (523.87 μm). The T4 polymer fibrous matrix seems to have the highest dimensional stability, which means that air-plasma on both faces of the material may lead to better comfort-related properties. From *Figure 11* and *Table III* and *Table IV*, from the analyses of surfaces with the papillary sensor, the polymer fibrous matrix T4 has the highest roughness level, meaning 719 μm, almost three times higher than the roughness of the other polymer fibrous knitted structures. We can assume that the most intense massaging effect is offered by the sample with the highest roughness level, measured with the papillary sensor, meaning the T4 polymer fibrous knitted structure. As a result of the analyses of the sample surface by scanning with the ball sensor, the T4 sample has the highest roughness value, meaning 894 μm, which is almost equal to that of the T5 knitted sample - 893 μm.

CONCLUSION
The effect of air-plasma surface modification on the deformation response of bamboo derived cellulosic fibrous systems and the optimization of their 3D surface structure to enhance comfort-related properties proved to be substantial. The surface modifications induced by air-plasma treatment are in a good correlation with the mechanical behavior. The roughness levels of the samples studied using the ball sensor are higher than those of the specimens scanned using the papillary sensor. The T4 sample has the lowest deformation (45.81 μm) and total deformation (523.87 μm) compared with the other systems, meaning that sample T4 has the highest dimensional stability.

REFERENCES

[1] EN ISO 4287: Geometrical Product Specifications (GPS). Surface texture: Profile method – Rules and procedures for the assessment of surface texture (1996).

[2] Guignard Iorgoaiea M., Campagne C., Giraud S, Brebu M., Vrinceanu N., Cioca L. I.: Functionalization of a bamboo knitted fabric using air plasma treatment for the improvement of microcapsules embedding, Journal of Textile Institute, 106 (2015) DOI: 10.1080/00405000.2014.942115.

[3] Hua Z.Q., Sitaru R., Denes F., Young R.A.: Mechanisms of oxygen- and argon- RF-plasma induced surface chemistry of cellulose, Plasmas and Polymers, 2, 196-220 (1997).

[4] Zemljic L.F., Persin Z., Stenius P.: Improvement of chitosan absorption onto cellulosic fabrics by plasma treatment, Biomacromolecules, 81, 199-202 (2011).

[5] Chan C.M.: Polymer surface modification and characterization. Carl Hanser Verlag, Munich (1994).

[6] Pandiyaraj N.K., Selvarajan V.: Non-thermal plasma treatment for hydrophilicity improvement of grey cotton fabrics, Journal of Materials Processing Technology, 199, 130-139 (2008).

[7] Morales J., Olayo M.G., Cruz G.J., Herrera-Franco P., Olayo R.: Plasma modification of cellulose fibers for composite materials, Journal of Applied Polymer science, 101, 3821-3828 (2006).

[8] Mozetic M.: Characterization of reactive plasmas with catalytic probes, Surface Coating Technology, 201, 4837-4842 (2007).

[9] Marcandalli B., Riccardi C.: Plasma technologies for textiles. Woodhead Publishing Ltd, Cambridge, (2007).

[10] Bennisch J.: Plasma processing of polymers. Dordrecht: Kluwer Academic Publishers, (1997).

[11] Titov V.A., Rybkin V.V., Shikova T.G., Ageeva T.A., Golubchikov O.A., Choi H.S.: Study on the application possibilities of an atmospheric pressure glow discharge with liquid electrolyte cathode for the modification of polymer materials, Surface Coating Technology, 199, 231-236 (2005).

[12] Titov V.A., Shikova T.G., Rybkin V.V., Smirnov D.S., Ageeva T.A., Choi H.S.: Modification of polyethylene, polypropylene and cotton using atmospheric pressure glow discharge with liquid electrolyte cathode, High Temp Mater Processes, 10, 467-478 (2006) DOI: 10.1615 / High Temp Mat Proc.v10.i3.100.

[13] Canal C., Erra P., Molina R., Bertrán E.: Regulation of surface hydrophilicity of plasma treated wool fabrics, Textile Research Journal, 8 (2007) DOI: 10.1177/0040517507078062.

[14] Choi H.S., Rybkin V.V., Titov V.A., Shikova T.G., Ageeva T.A.: Comparative actions of a low pressure oxygen plasma and an atmospheric pressure glow discharge on the surface modification of polypropylene, Surface Coating Technology, 200 (14), 4479-4488 (2006).

[15] Vesel A., Mozetic M., Hladnik A., Dolenc J., Zule J., Milosevic S.: Modification of ink-jet paper by oxygen-plasma treatment, Journal of Physics D: Applied Physics 40 (12), 3689, (2007).

[16] Gorjanc M., Bukosek V., Gorensek M., Vesel A.: The influence of water vapor plasma treatment on specific properties of bleached and mercerized cotton fabric, Textile Research Journal 80, 557-567 (2010).

[17] Ceria A., Rovero G., Sicardi S., Ferrero S.F.: Atmospheric continuous cold plasma treatment: Thermal and hydrodynamical diagnostics of a plasma jet pilot unit, Chemical Engineering and Processing: Process Intensification, 49(1), 65-69 (2010)DOI:10.1016/j.cep.2009.11.008.

[18] Cavanagh H.M.A., Wilkinson J.M.: Antibacterial activity of essential oils from Australian native plants, Phytotherapy research, 19 (7), 643-646 (2005).

[19] Cavanagh H.M.A., Wilkinson J.M.: Biological activities of lavender essential oil, Phytotherapy Research, 16, 301-308 (2002).

[20] Guo L., Campagne C., Perwuelz A., Leroux F.: Zeta potential and surface physico-chemical properties of atmospheric air-plasma treated PET fabrics, Textile Research Journal, 79, 1371-1377 (2009).

[21] Leroux F., Perwuelz A., Campagne C., Behary N.: Atmospheric air-plasma treatments of polyester textile structures, Journal of Adhesion Science and Technology, 20, 939-957 (2006).

[22] EN ISO 105-C06: Textiles-Tests for fastness-part C06. Colour fastness to domestic and commercial laundering (2005).

[23] Ribitsch V., Stana-Kleinscheck K.: Characterizing textile fiber surfaces with streaming potential measurements, Textile Research Journal, 68, 701-707 (1998).

[24] Grundke K., Jacobasch H.J., Simon F., Schneider S.T.: Surface characterisation of polymers by physicochemical measurements, Journal of Adhesives Science Technology 48, 57-73 (1995).

AUTHORS' ADDRESSES
Narcisa Vrinceanu
Valentin Dan Petrescu
Dan Dumitru Dumitrascu
Diana Coman
Lucian Blaga University of Sibiu
Faculty of Engineering
Department of Industrial Machines and Equipment
2-4 Emil Cioran Street
500204, Sibiu
ROMANIA

Mirela Iorgoaiea Guignard
Gheorghe Asachi Technical University of Iaşi
53 Mangeron Street
700205, Iasi
ROMANIA

Christine Campagne
University Lille Nord France
Roubaix
FRANCE

Gemtex, Ensait
Roubaix
FRANCE

Stephane Giraud
ENSAIT, Lab Genie Mat Text GEMTEX
Roubaix
FRANCE

Raluca Ioana Prepelita
University of Medicine and Pharmacy of Iaşi
Faculty of Medicine
Department of Psychiatry
16 Universitatii Street
700115, Iasi
ROMANIA

Noureddine Ouerfelli
Imam Abdulrahman Alfaisal University
Department of Chemistry
College of Science
P.O. Box 1982
Dammam 31441
SAUDI ARABIA

Université de Tunis El Manar
Institut Supérieur des Technologies Médicales de Tunis
LR13SE07, Laboratoire de Biophysique et Technologies Médicales
9 Avenue Dr.
Zouhaier Essafi 1006 Tunis
TUNISIA

Mirela Petruta Suchea
Center of Materials Technology and Laser
School of Electrical Engineering
Technological Educational Institute of Crete
Heraklion
GREECE

National Institute for Research and Development in Microtechnologies (IMT-Bucharest)
126 A, Erou Iancu Nicolae Street
P.O. Box 38-160
023573 Bucharest
ROMANIA